

Ultraluminous Extragalactic Chemistry

Sergio Martín Ruiz^{1,2}

¹European Southern Observatory,
Alonso de Córdova 3107, Vitacura, Casilla 19001, Santiago 19, Chile

²Joint ALMA Observatory,
Alonso de Córdova 3107, Vitacura, Casilla 19001, Santiago 19, Chile
email: smartin@eso.org

Abstract. At a distance of 77 Mpc, the Ultraluminous galaxy Arp 220 is the closest extragalactic equivalent to Galactic hot cores. The low resolution SMA survey showed a highly excited confusion limited spectrum. The new ALMA snapshot spectral scan opens the possibility of chemically resolve the two nuclei at unprecedented sensitivity. When completed, it will be the widest survey ever done towards an extragalactic object. The model of Band 6 and 7 data already shows the chemical similarities between the interacting nuclei which may provide clues on the similar heating sources. Vibrationally excited transitions may be tracing the deeply embedded dust obscured active nuclei and/or hot compact star burst. This vibrational emission is the brightest ever measured in an extragalactic object, and even so compared with Galactic hot cores. In fact, the eastern one is the brightest in such vibrational emission. Water mega-maser emission also points towards a very compact sources likely related to star forming clumps within both Arp 220 nuclei.

Keywords. ISM: molecules, galaxies: abundances, galaxies: active, galaxies: starburst, galaxies: individual (Arp 220)

1. Introduction

During the last decade the increased receiver bandwidth in state of the art millimeter and submillimeter telescopes has allowed a rapid increase in the observations of unbiased line surveys in the extragalactic interstellar medium. Table 2 in Martín (2011) summarized some of the ongoing observational efforts, some of which have been recently published (Aladro *et al.* 2011, 2015; Davis *et al.* 2013; Watanabe *et al.* 2014, 2016). The increasing number of such unbiased surveys allows comparative studies between the nuclear region of galaxies dominated by different types of activity (Aladro *et al.* 2015).

Obviously, the advent of high sensitivity instruments like ALMA is having a transformational impact in the field of extragalactic astrochemistry both through unbiased line surveys (Costagliola *et al.* 2015; Muller *et al.* 2014b,a, 2016) and deep multi molecular observations towards nearby galaxies (Meier *et al.* 2015; Martín *et al.* 2015; Nakajima *et al.* 2015; Tosaki *et al.* 2017).

These high sensitivity observations are demonstrating the potential to investigate deeply buried galactic nuclear regions through unbiased molecular observations. In particular it may an unique tool to the study the obscured nuclei of luminous and ultraluminous galaxies. These galaxies are radiating most of their energy as thermal dust emission in the infrared and they are the dominant contribution to the star formation rate at $z > 2$ (Madau & Dickinson 2014). Some of these objects are observed to be extremely compact where most of their luminosity is observed to emerge within a few tens of parsecs nuclear region (Aalto *et al.* 2015b; Costagliola *et al.* 2015; Martín *et al.* 2016). Their nuclear power source, embedded inside obscurations of $A_v > 1000$ mag and thus

obscured at almost everywavelength, prevent us from determining their nature. In most cases, the presence of a dominating AGN or a hot starburst in an intense and compact mode cannot be differentiated (Aalto *et al.* 2015b).

2. ULIRG chemistry of embedded nucleus: Arp 220

Arp 220, at a distance of ~ 77 pc, is the prototype of ULIRG, in a later merging state showing two deeply buried nuclei separated by $\sim 1''$ (Sakamoto *et al.* 1999). The nuclei are optically thick outside the range of 5 – 350 GHz (Barcos-Muñoz *et al.* 2015). Arp 220 has been observed with almost any instrument available but the nature of its nuclear powering source is still debated. This galaxy has been the subject of many recent studies with ALMA during its first observing cycles (Rangwala *et al.* 2015; Scoville *et al.* 2015, 2017; Zschaechner *et al.* 2016; Martín *et al.* 2016; König *et al.* 2017).

The presence of an AGN in its nuclei has been claimed based on the detected hard X-ray point source towards the western nucleus and softer emission towards the eastern one Clements *et al.* (2002), as well as the large equivalent width of the Fe 6.7 keV line (Teng *et al.* 2009). However its starburst contribution is evidenced by the dozens of SN remnants towards both nuclei, with a SN rate consistent with the SFR derived from FIR observations (Lonsdale *et al.* 2006; Parra *et al.* 2007). Similarly the extended faint soft X-ray emission may be starburst driven (McDowell *et al.* 2003).

In order to establish whether the effect of the inner powering source had an imprint on the molecular composition in the ISM Martín *et al.* (2011) carried out an unbiased line survey at 1.3 mm with the SMA which resulted in no obvious evidence from an AGN on the observed molecular abundances. In fact, the vibrationally excited transitions of HC₃N, together with the large abundance of water based on the isotopologues ratio H₂¹⁸O/C¹⁸O, were claimed to be evidences of a compact concentration of $\sim 10^6$ hot cores within the inner 700 pc of Arp 220.

It is worth mentioning that the unbiased line survey carried out with ALMA towards the also compact obscured nuclei in the LIRG NGC 4418 showed molecular abundances resembling closely those of Arp 220 (Costagliola *et al.* 2015).

3. Dissecting the two nuclei of Arp 220 with ALMA

Since the resolution achieved with the SMA observations was around 700 pc, it was not possible to disentangle the emission from the individual nuclei. Thus we made use of the unprecedented sensitivity and resolution of ALMA to study the individual molecular emission from the two nuclei in Arp 220. At a resolution of $0.5''$, we scanned the atmospheric bands 6 and 7 in Cycle 1, and the bands 3 and 4 in Cycle 3. The observations covered the frequency range from 86 to 363 GHz, which, when completed, will result in the widest unbiased scan towards an extragalactic source. It is worth noting that the scan consisted of snapshot observations of 2-4 min at the higher bands and 8-20 min in the lower, in order to achieve an homogeneous noise level of 2mJy and 1mJy, respectively.

Figure 1 shows the observed spectrum towards the western nucleus and the modeled synthetic spectrum fitted to the data. The large line width of ~ 300 km s⁻¹ results in a heavily blended spectrum where the model includes 1331 transitions with flux densities above 1σ . The eastern nucleus, though generally fainter, still shows a heavily blended spectrum.

As shown in the Figure 1, modeling the data is particularly tricky due to the fact that almost all spectral features show a heavy absorption in the center. This was clearly shown in the study of HCN and HCO⁺ emission by Martín *et al.* (2016) which showed

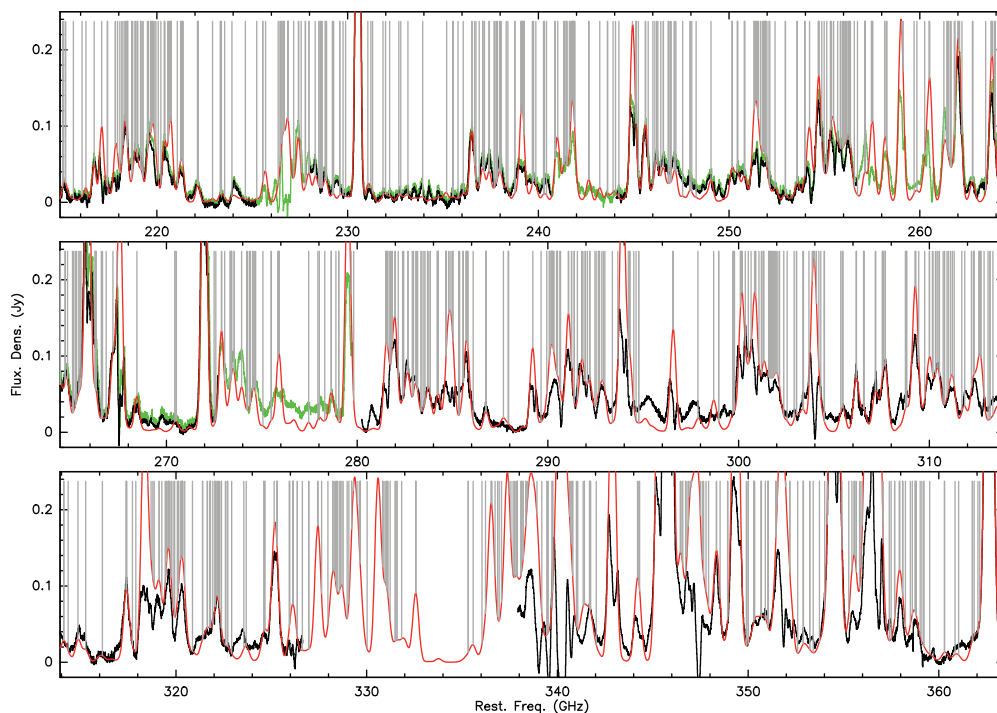


Figure 1. Full band 6 and 7 spectral coverage with ALMA towards its western nucleus. Black line shows the observed spectrum at $0.65''$ while the green section shows observation at coarser resolution. The model is shown in red and the grey vertical lines show the location of all the spectral features used in the model (Martín *et al.* In preparation)

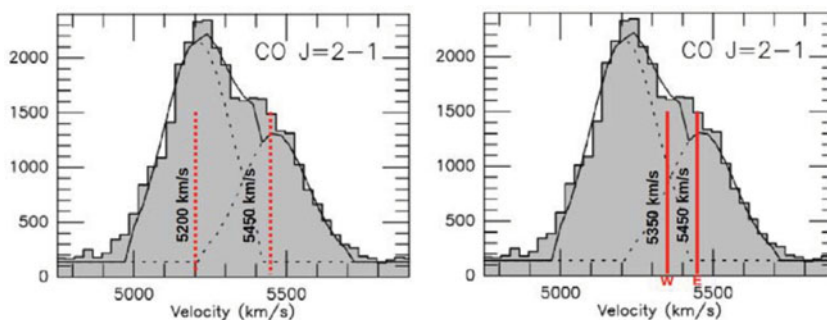


Figure 2. (LEFT) Double Gaussian fit used by Martín *et al.* (2011) to disentangle the two Arp 220 nuclei in velocity. This velocity identification may not be adequate as shown in the right panel. (RIGHT) Systemic velocity of the two nuclei as resulting from an absorbed Gaussian fit to the individual spectra of the two nuclei.

multiple absorption systems in the line of sight of both nuclei where approximately 70% of the line emission is absorbed. Thus the model fit was performed making use of the profile outside the absorbed region which implies a significant level of uncertainty and explains why most of model in Figure 1 falls above the observed spectrum.

The fit of absorbed Gaussian profiles to these lines was in agreement with previous estimates of the individual systemic velocities of both nuclei. It clearly shows that, as sometimes done in the literature, the use of a double Gaussian fit to unresolved spectral

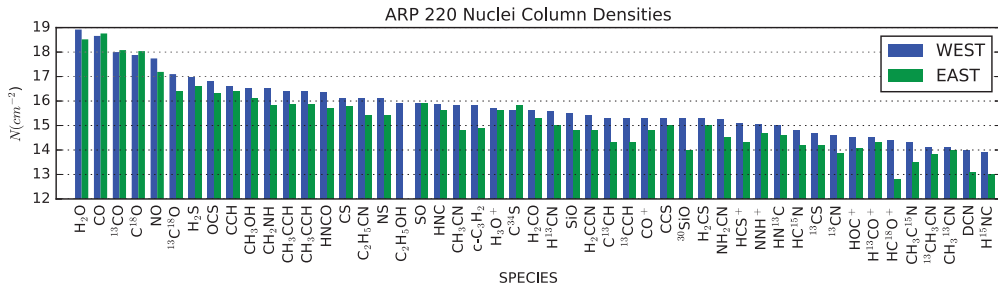


Figure 3. Comparison between the absolute column densities of all detected species in the two nuclei of Arp 220. Figure extracted from Martín *et al.* In prep.

observations as a way to separate the two nuclei in velocities (Greve *et al.* 2009; Martín *et al.* 2011) may not be adequate. This difference is shown in Figure 2.

Based on the modeled spectra, column densities of 49 molecular species, including some isotopologues, were calculated for the individual nucleus. Figure 3 shows a preliminary comparison based on these derived column densities. Within a factor of 3, no significant or obvious molecular trend is found to differentiate the nuclei. This result indicates that either there is no molecular fingerprint due to the putative AGN in the western nucleus or that such is already diluted at 240 pc resolution.

4. The vibe of Arp 220

One of the most interesting spectral features in the Arp 220 scan are the brightness of its vibrationally excited transitions.

After the first detection of vibrationally excited absorption of HCN by Salter *et al.* (2008), a number of vibrational transitions of HCN and HC₃N have been reported towards LIRGs (Sakamoto *et al.* 2010; Costagliola & Aalto 2010; Costagliola *et al.* 2015) and ULIRGs (Martín *et al.* 2011; Imanishi & Nakanishi 2013; Aalto *et al.* 2015a,b). These transitions require of mid-IR photons stemming from heated dust with $T_d > 100$ K to be efficiently pumped (Sakamoto *et al.* 2010; Aalto *et al.* 2015b). All the sources where this emission is been observed share a large luminosity within a very compact nuclear region (Aalto *et al.* 2015b). However, though a very compact concentration of gas and a high temperature gradient is required to explain the observed emission, it is uncertain whether this vibrational transitions are excited in the surroundings of an AGN or due to a compact hot star forming event.

Though the sample of detected sources is still limited, a lot of observational efforts are ongoing to expand the range of sources and luminosities (Imanishi & Nakanishi 2014; Imanishi *et al.* 2016).

Martín *et al.* (2016) presented for the first time high resolution observations of the vibrational emission where the two nuclei were resolved from each other. The emission is observed to be at the systemic velocity of each nucleus, and although not resolved, it appears to be coming from a region smaller than the resolved extended continuum emission.

It is worth noting that, as shown in Figure 4, the nuclei in Arp 220 show the highest ratio between the luminosity of the vibrational emission of HCN and the infrared luminosity. This ratio, measured with both the $J = 3 - 2$ and $4 - 3$ HCN vibrational transitions, is higher than any other extragalactic source and one order of magnitude above what is observed in Galactic hot cores. Also interesting is the fact that among the two nuclei, the eastern one is showing the highest ratio. So if this emission is AGN

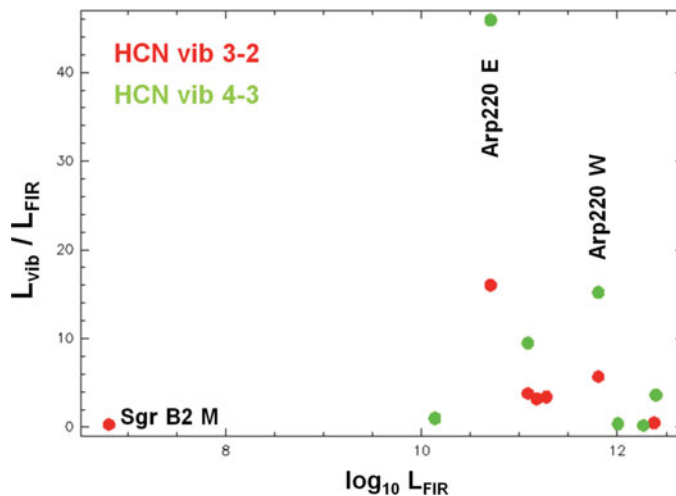


Figure 4.

powered, this effect is more prominent towards the eastern nucleus and to a lesser degree in the western, where the putative AGN is placed.

5. Resolved water “mega-maser” in Arp 220

The ALMA spectral scan of Arp 220 also covered the 325 GHz transition of water. The water emission has been claimed to be of maser origin despite the lack of line variability and showing a line shape similar to any other species (Cernicharo *et al.* 2006). König *et al.* (2017) compiled the 325 GHz in the ALMA survey together with the 22 GHz VLA detection by Zschaechner *et al.* (2016) and the Band 5 science verification data. All these observations had a similar resolution of $\sim 0.7''$ which was enough to separate the emission from both nuclei.

Line blending in Arp 220 is particularly an issue. Indeed all 3 transitions are significantly affected by blending (see figures in Zschaechner *et al.* 2016; König *et al.* 2017). The 22 GHz was seen to emit right within the NH_3 profile. The ammonia contribution was subtracted by using the line profile of nearby ammonia transitions. In the case of the 180 GHz and 325 GHz, the de-blending was carried out by subtracting the synthetic profile fitted to the whole spectral scan. In the case of the 325 GHz transition, the line is falling within the range of the scan. However, the modeled spectra had to be extrapolated down to the 180 GHz transition, but still Figure 1 in König *et al.* (2017) shows that the agreement between the “preliminary” model and the observed profile is good, in particular towards the western nucleus. Additionally the de-blended line profiles show a good agreement in shape between the 180 and 325 GHz transition.

Despite the non variability of the water emission is confirmed over a one decade period, line intensities do not agree with a thermal origin. Also, the modeling suggests a very compact origin of the emission, which could stem from a large number of star-forming clumps. These clumps might be the origin of an isotropically distributed maser emission, required to explain the non variability of the line profile, in both nuclei of Arp 220.

References

Aalto, S., Garcia-Burillo, S., Muller, S., *et al.* 2015a, *A&A*, 574, A85

- Aalto, S., Martín, S., Costagliola, F., *et al.* 2015b, *A&A*, 584, A42
- Aladro, R., Martín, S., Martín-Pintado, J., *et al.* 2011, *A&A*, 535, A84
- Aladro, R., Martín, S., Riquelme, D., *et al.* 2015, *A&A*, 579, A101
- Barcos-Muñoz, L., Leroy, A. K., Evans, A. S., *et al.* 2015, *ApJ*, 799, 10
- Cernicharo, J., Pardo, J. R., & Weiss, A. 2006, *ApJ*, 646, L49
- Clements, D. L., McDowell, J. C., Shaked, S., *et al.* 2002, *ApJ*, 581, 974
- Costagliola, F. & Aalto, S. 2010, *A&A*, 515, A71
- Costagliola, F., Sakamoto, K., Muller, S., *et al.* 2015, *A&A*, 582, A91
- Davis, T. A., Heiderman, A., Evans, N. J., & Iono, D. 2013, *MNRAS*
- Greve, T. R., Papadopoulos, P. P., Gao, Y., & Radford, S. J. E. 2009, *ApJ*, 692, 1432
- Imanishi, M. & Nakanishi, K. 2013, *AJ*, 146, 91
- Imanishi, M. & Nakanishi, K. 2014, *AJ*, 148, 9
- Imanishi, M., Nakanishi, K., & Izumi, T. 2016, *ApJ*, 825, 44
- König, S., Martín, S., Muller, S., *et al.* 2017, *A&A*, 602, A42
- Lonsdale, C. J., Diamond, P. J., Thrall, H., Smith, H. E., & Lonsdale, C. J. 2006, *ApJ*, 647, 185
- Madau, P. & Dickinson, M. 2014, *ARAA*, 52, 415
- Martín, S. 2011, in: J. Cernicharo & R. Bachiller (eds.), *The Molecular Universe*, Proc. IAU Symposium No 280 p. 351
- Martín, S., Aalto, S., Sakamoto, K., *et al.* 2016, *A&A*, 590, A25
- Martín, S., Kohno, K., Izumi, T., *et al.* 2015, *A&A*, 573, A116
- Martín, S., Krips, M., Martín-Pintado, J., *et al.* 2011, *A&A*, 527, A36
- McDowell, J. C., Clements, D. L., Lamb, S. A., *et al.* 2003, *ApJ*, 591, 154
- Meier, D. S., Walter, F., Bolatto, A. D., *et al.* 2015, *ApJ*, 801, 63
- Muller, S., Black, J. H., Guélin, M., *et al.* 2014a, *A&A*, 566, L6
- Muller, S., Combes, F., Guélin, M., *et al.* 2014b, *A&A*, 566, A112
- Muller, S., Müller, H. S. P., Black, J. H., *et al.* 2016, *A&A*, 595, A128
- Nakajima, T., Takano, S., Kohno, K., *et al.* 2015, *PASJ*, 67, 8
- Parra, R., Conway, J. E., Diamond, P. J., *et al.* 2007, *ApJ*, 659, 314
- Rangwala, N., Maloney, P. R., Wilson, C. D., *et al.* 2015, *ApJ*, 806, 17
- Sakamoto, K., Aalto, S., Evans, A. S., Wiedner, M. C., & Wilner, D. J. 2010, *ApJ*, 725, L228
- Sakamoto, K., Scoville, N. Z., Yun, M. S., *et al.* 1999, *ApJ*, 514, 68
- Salter, C. J., Ghosh, T., Catinella, B., *et al.* 2008, *AJ*, 136, 389
- Scoville, N., Murchikova, L., Walter, F., *et al.* 2017, *ApJ*, 836, 66
- Scoville, N., Sheth, K., Walter, F., *et al.* 2015, *ApJ*, 800, 70
- Teng, S. H., Veilleux, S., Anabuki, N., *et al.* 2009, *ApJ*, 691, 261
- Tosaki, T., Kohno, K., Harada, N., *et al.* 2017, *PASJ*, 69, 18
- Watanabe, Y., Sakai, N., Sorai, K., Ueda, J., & Yamamoto, S. 2016, *ApJ*, 819, 144
- Watanabe, Y., Sakai, N., Sorai, K., & Yamamoto, S. 2014, *ApJ*, 788, 4
- Zschaechner, L. K., Ott, J., Walter, F., *et al.* 2016, *ApJ*, 833, 41